Journal of Statistical Physics, Vol. 109, Nos. 3/4, November 2002 (© 2002)

Strong and Weak Damping in the Adiabatic Motion of the Simple Piston

G. P. Morriss[1] and Ch. Gruber[2]

Received December 20, 2001; accepted March 25, 2002

We investigate the microscopic mechanisms associated with strong and weak damping in the adiabatic motion of the simple piston with finite mass and finite amount of gas. The velocity of the piston relative to the thermal velocity of the gas particles is the principal factor in determining the behaviour. When the piston velocity is always smaller than the thermal velocity we observe weak damping. When it is greater than the thermal velocity for part of its motion there is strong damping.

KEY WORDS: Damping; adiabatic; piston.

1. INTRODUCTION

The "adiabatic piston" is a classic textbook example of a problem which can not be solved using the two laws of thermostatics. The system consists of a finite cylinder containing two gases separated by a movable adiabatic piston. Initially the two gases are in thermal equilibrium and the piston is fixed. The problem is to study the time evolution, and the final state, when the piston is free to move.[(1)] Recently this problem was investigated using the Boltzmann equation,[(2)] the Liouville equation[(3)] as well as using numerical simulation. It is now clear that the evolution of the piston proceeds in two stages with time scales which are very different if the mass of the gas molecules is much smaller than the mass of the piston. In the first stage the evolution of the piston is deterministic and the system evolves adiabatically (no heat transfer from one gas to the other) toward a state of mechanical equilibrium (equal pressures on both sides). On the other hand

[1] School of Physics, University of New South Wales, UNSW Sydney NSW 2052, Australia; e-mail: G.Morriss@unsw.edu.au

[2] Institut de Physique Théorique, École Polytechnique Fédérale de Lausanne, CH-1015 Lausanne, Switzerland.

0022-4715/02/1100-0549/0 © 2002 Plenum Publishing Corporation

in the second stage the evolution is stochastic; this stochastic behaviour induces a heat transfer which then leads to thermal equilibrium.

Although the second stage, which proceeds on a very large time scale, is qualitatively rather well understood,[4] the same is not true for the first stage (i.e., for the adiabatic evolution). To gain insight into the adiabatic evolution we have investigated the "simple piston" problem, that is just one gas in a container with a piston which exerts a constant external force (Fig. 1). This system does not exhibit the difficulties associated with the adiabatic piston, and one easily deduces the final equilibrium state from the two laws of thermostatistics. Experimentally this problem has been introduced in 1929 as a method for measuring the ratio of the specific heats c_p/c_v of a gas.[5] Recently new and unexpected results were observed which indicate very different behaviour depending on whether the damping is weak or strong.[6] If the piston motion is slow enough, the gas in the cylinder is in a quasi-static state and one can assume that the process is isoentropic. This is what has been assumed in Rüchardt's experiment in 1929, and has been confirmed by recent experiments in the case of weak damping.[6] However, for strong damping the recent experimental results clearly indicate that the assumption of adiabatic oscillations is no longer valid. In a recent paper[7] we have investigated this simple piston. If the system is considered in the thermodynamic limit, where the dimensions of the cylinder ($X(t)$, L), the number of gas molecules N, and the mass M of the piston are all infinite (with M/L, and $LX(t)/N$ finite), then the problem can be easily discussed since recollisions of gas molecules on the piston can be neglected (at least at low enough densities). On the other hand the case of a finite cylinder with finite N and M is much more difficult since now recollisions are the essential mechanism. We have studied the simple piston in two-dimensions, from both a kinetic theory approach

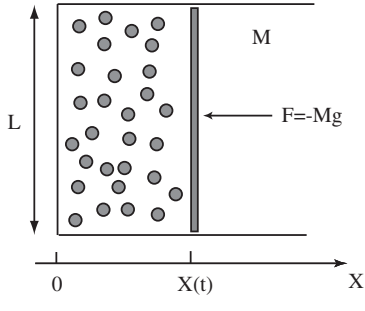

Fig. 1. The geometry for the adiabatic piston experiment is a cylinder of width $L = 470.302$ containing 1728 hard disks, enclosed by a piston of mass M with initial position $X(0) = 73.485$.

using the Boltzmann equation, and by direct molecular dynamics simulation of a system with hard disk particles and rigid walls for both the walls of the cylinder and the face of the piston. The observed motion of the piston can very often be considered (to a good approximation) to be the motion of a damped oscillator, with a characteristic frequency ω and damping coefficient λ. In this work we identified "weak" and "strong" damping regimes.

We consider two initial states with the same geometry (cylinder and position of the piston, Fig. 1), the same number of particles, temperature, and external force, but different values of the piston mass M (and thus different values of g, chosen such that Mg is fixed). The system is two-dimensional and the fluid consists of 1728 hard disks of unit diameter. The initial position of the piston is $X(t=0) = 73.485$ (with $L = 470.302$) corresponding to an initial number density of 0.05. The initial temperature is $kT = 10$ and the external force is $F = -Mg = 3200$. Taking Enskog's expression for the pressure, $p = 0.5418$, while the external pressure is $F/L = -6.804$. Therefore the external force is larger than the force exerted by the fluid and the piston evolves to the final state $X_j = 42.23$, $kT_j = 67.88$ which is independent of M.

The characteristic feature of strong damping is best illustrated in Fig. 2. In the first frame the temperature after one cycle of the piston motion has changed from $kT = 10$ to $kT = 14$. Thus only a small amount of energy has been transferred from the piston to the gas. In the second frame, the strong damping state, in one cycle the temperature has increased from $kT = 10$ to $kT = 42$. Thus in only one cycle the strong damping state has transferred more than 50% of the energy from the piston to the gas. Similarly the increase in the entropy is much higher in the second frame.

2. MECHANISMS

In this paper we consider two initial states which typify the two damping regimes. For the strong damping state we take a piston mass $M = 100$ and $g = 32$, and for the weak damping state we take a piston mass $M = 8000$ and $g = 0.4$ (thus the forces Mg are the same). The initial temperatures are both $kT = 10$, and the final equilibrium positions are the same ($X_f = 42.23$ and $kT_f = 67.88$), thus the only difference is in the approach to the final position. In what follows, we refer to states by specifying (kT, M, g), for example (10, 100, 32) for the strong damping state. Movies of the two states show that the strong damping state has an obvious wave develop in front of the piston as it moves down the cylinder for the first time. In the weak damping case there is no such obvious wave motion. These observations lead us to investigate microscopic motion in

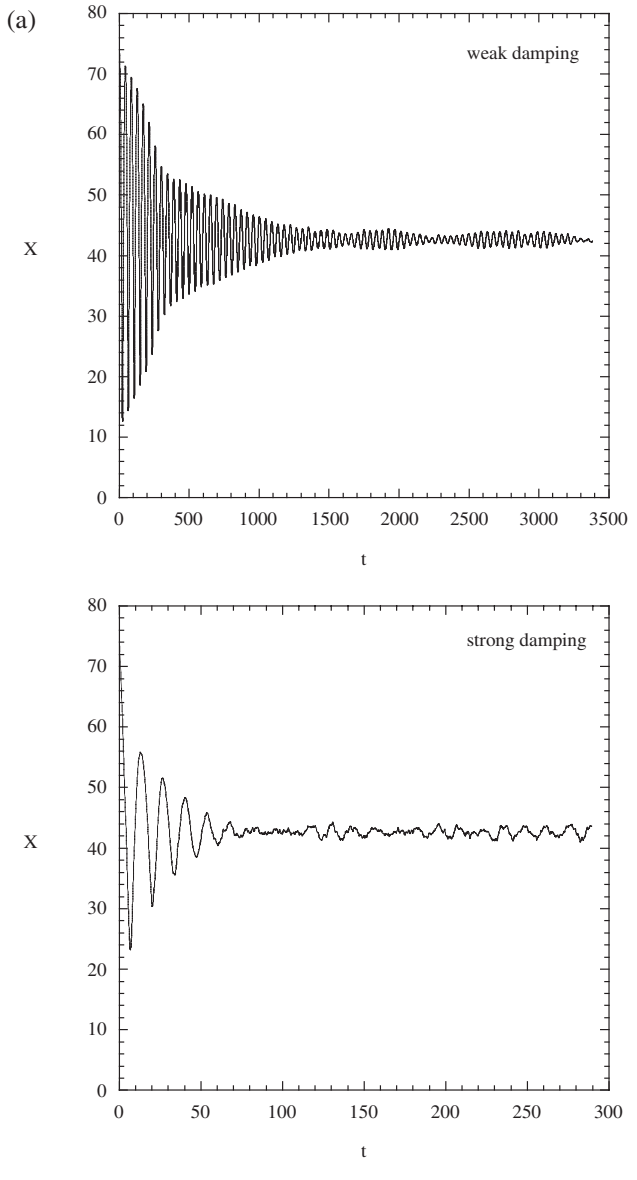

Fig. 2. (a) The position of the piston as a function of time for weak damping $\lambda/\omega \approx 0.014$, and then strong damping $\lambda/\omega \approx 0.082$. (b) The x (dashed line) and y (solid line) temperatures as a function of time during the first two cycles of the piston motion. The most obvious difference between the strong and weak damping regimes is that in the weak damping case more of the internal energy is returned to the piston motion. Note that $kT_\alpha = \frac{1}{N}\sum_i mv_{\alpha i}^2$ where $\alpha = x$, y, and $kT = \frac{1}{2}(kT_x + kT_y)$.

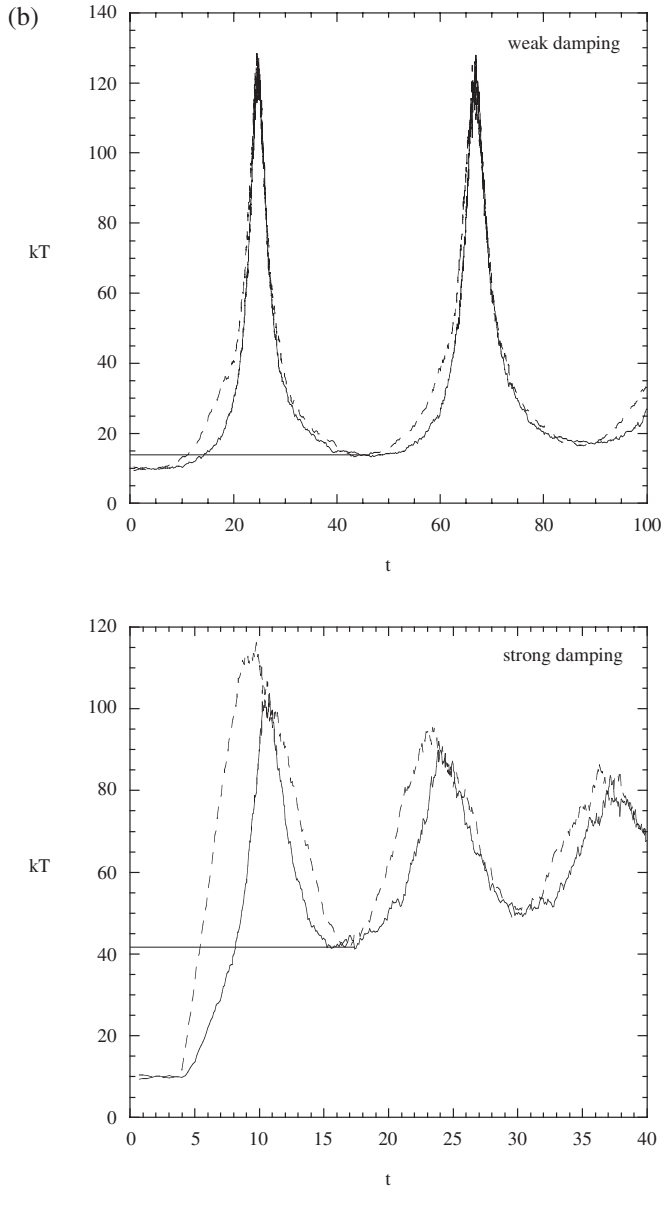

Fig. 2. *(Continued)*.

more detail looking at the number density and momentum density as a function of position, between the bottom of the cylinder and the piston. In much of what follows, we restrict our consideration to the first few cycles of the piston motion because the differences in the damping rates are evident very quickly.

2.1. Strong Damping Case

Our initial configuration of disks in the cylinder is allowed to thermalise for 2000 collisions and then the piston is released. For both the strong and weak damping cases this corresponds to a time of $t = 3.68$. The simulation then continues until the new equilibrium is reached (or some fluctuating state whose mean is the new equilibrium, see Fig. 2a).

Another way of seeing the effect of strong damping is to consider the zeroth velocity moment $j_0(t)$, defined as

$$j_q(t) = \frac{(-1)^q}{q!} \int_0^\infty dv\, \varphi(v, t)\, v_q \tag{1}$$

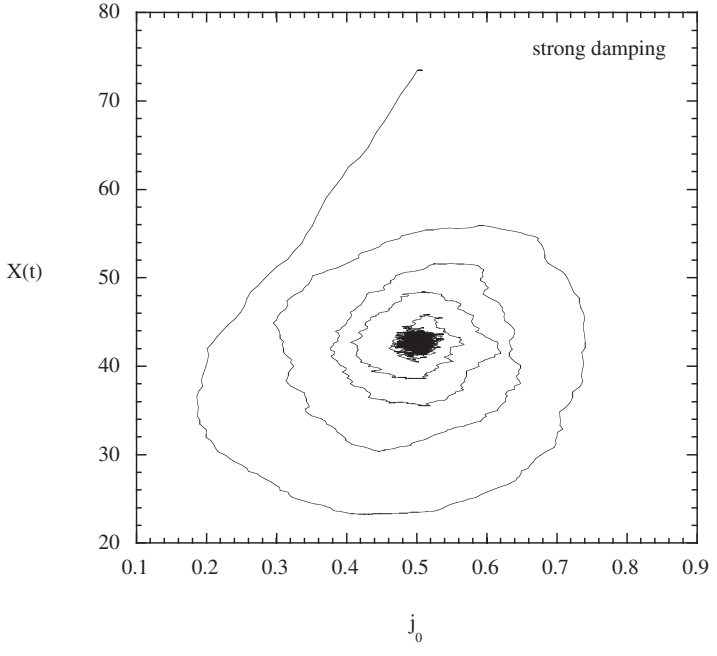

Fig. 3. The piston motion versus the zeroth velocity moment which shows a strongly damped motion towards an equilibrium position at $J_0(t) = \frac{1}{2}$. The initial straight segment from $X(0) = 73.4$ to $X = 42$ is different in character to the subsequent motion.

where $\varphi(v, t)$ is the velocity distribution at time t. $j_0(t)$ is the proportion of the gas particles that are moving toward to piston face. The plot of piston position $X(t)$ versus $j_0(t)$, in Fig. 3, shows an initial straight segment, then a fast spiralling motion toward the equilibrium point. The initial straight segment appears to be different in character to the subsequent piston motion. However, for the remainder of the motion $X(t)$ and $j_0(t)$ are correlated as they oscillate about their new equilibrium values.

Figure 4 shows the position and velocity of the piston over the first two cycles. After the piston is released, the initial descent is marked by an almost constant velocity $V \cong -8$ for a time of $t \cong 6$, and hence a linear displacement with time (this also corresponds to the linear segment in Fig. 3), i.e., the force exerted by the fluid on the piston is constant, equal to Mg. This is different from the behaviour of the piston in its second and subsequent descents. The second cycle of the piston motion is more regular with a steady change in velocity and associated change in position, i.e., the force exerted by the fluid is again constant, but smaller than Mg.

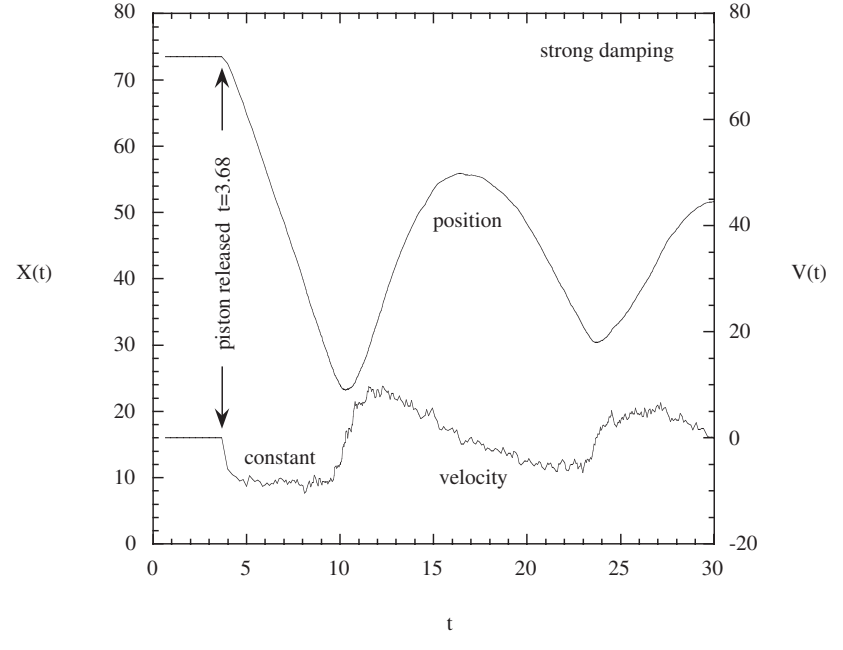

Fig. 4. The position and velocity of the piston as a function of time. The piston is released at $t = 3.68$ and reaches the bottom of its travel at $t = 10.48$. The piston reaches a velocity of $V \sim -8$ very quickly, then maintains that velocity until almost $t = 10.48$.

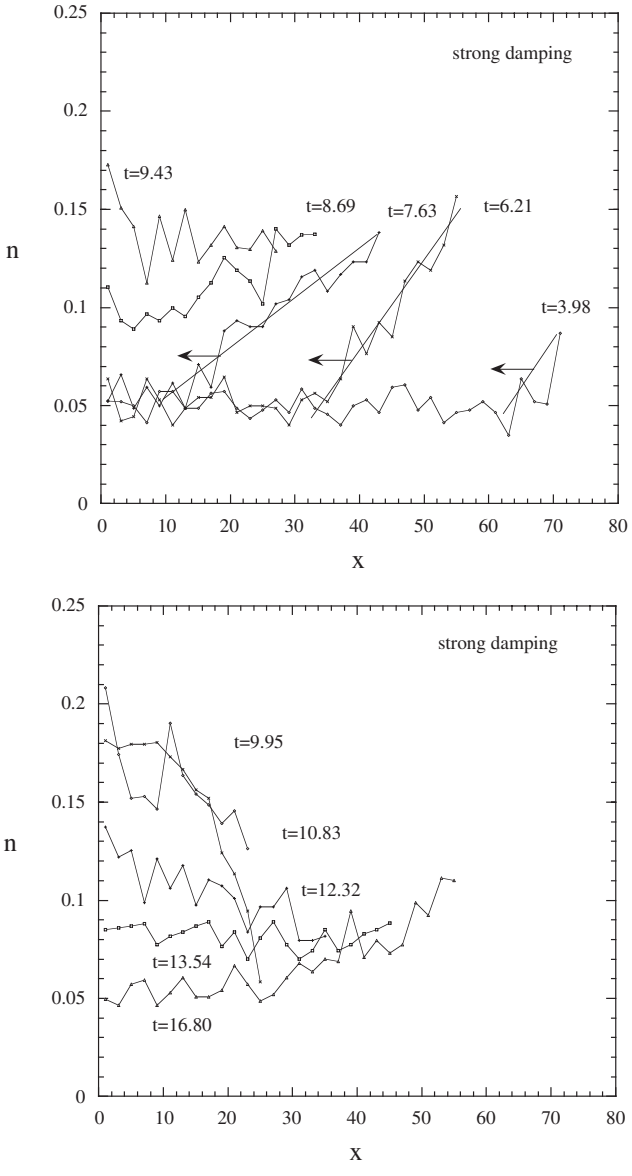

Fig. 5. The number density profiles at various times through the first descent of the piston for the strong damping state (the piston is released at $t = 3.68$). In the first few times there is good evidence of a bow-wave on the front of the piston.

2.2. Number Density Profiles

A movie of the piston motion shows that when the piston moves down for the first time it carries with it a dense region of particles within a small distance from the piston surface. The leading edge of this wave-like structure reaches the bottom of the cylinder before the piston reaches its lowest point. But when the piston begins moving up from its lowest point the fluid looks to have a more uniform density at each time, which is determined by the volume of the cylinder. There is no obvious wave like motion that could be considered to come from a reflection from the cylinder base, or no wave like motion in the second descent of the piston.

To look for more direct evidence of this wave motion, we construct number density profiles between the piston face (at the right-hand side) and the bottom of the cylinder (at $x = 0$) and we observe a triangular shaped wave in front of the piston. Initially the front of the wave travels faster ($v \sim -16$) than the piston ($V \sim -8$), in this case, so that the slope of the wave profile decreases with time. The wavefront reaches the wall just after $t = 7.63$, and then at $t = 9.43$ the density profile is essentially constant.

The piston reaches the bottom of its travel at $t = 10.48$, and the number density profile reaches a maximum before the piston begins to travel back up the cylinder. The density now begins to drop as the piston moves up and the total volume increases. However, the number density varies rather smoothly, with a maximum close to the bottom of the cylinder. The rising of the piston appears to be associated with a decrease in number density across the whole fluid, without any strongly localised motion or wave-like structure. Even at $t = 16.8$, the number density profile remains smooth, suggesting that the whole fluid is responding to the piston motion rather than a localised wave motion. However, it should be emphasised that the wavelength of a typical sound wave would be much larger than the dimensions of the simulation and would not appear to be a localised structure.

2.3. Instantaneous Pressure

The instantaneous pressure on the piston surface and the bottom of the cylinder is calculated as a function of time (Fig. 6). For the strong damping state the pressure on the piston surface increases immediately after the piston is released, but thereafter the pressure slightly decreases and remains relatively constant regardless of the piston position. The pressure on the bottom of the cylinder behaves quite differently. It is strongly peaked when the piston is at the lowest point of its motion, particularly for the first cycle, but also a similar effect is observed for the second cycle of the piston, as it should.

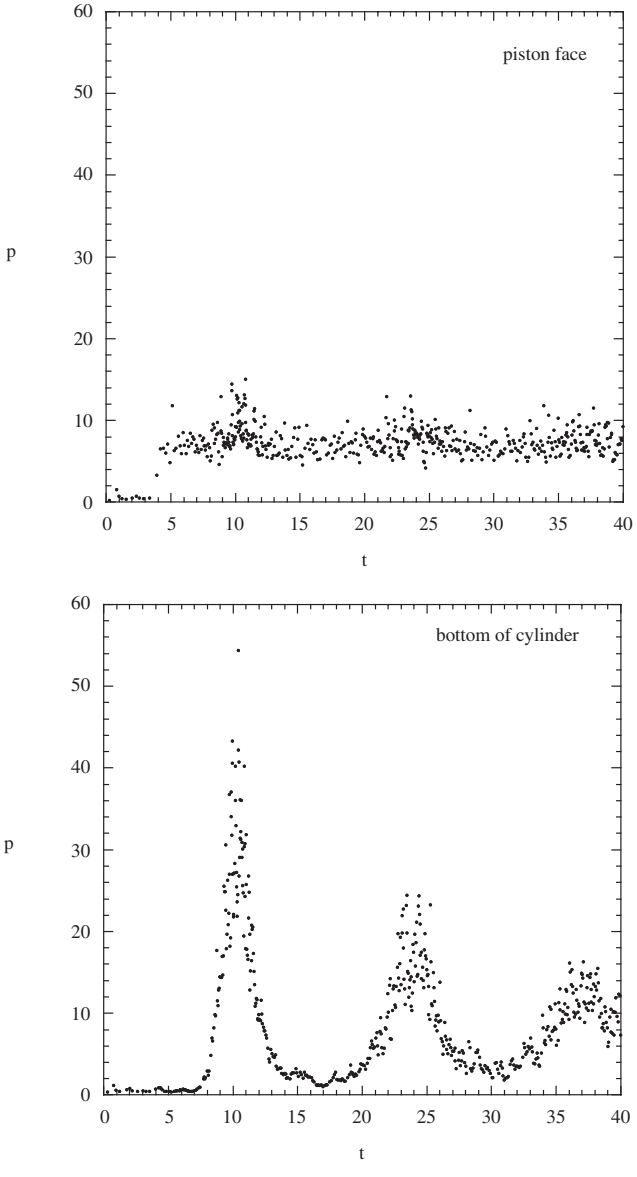

Fig. 6. For the strong damping state (10, 100, 32) the pressure on the bottom of the cylinder cycles with the motion of the piston, but the pressure on the piston face remains relatively constant.

For nearby strong damping states $(kT, M, g) = (10, 200, 16)$ & (10, 50, 64), the behaviour of the instantaneous pressures mirrors that of the state (10, 100, 32). The pressure on the piston surface is relatively constant, but the pressure on the bottom of the cylinder is peaked at the bottom of the piston motion. For the intermediate state (10, 800, 4), both pressures are peaked at the lowest point of the piston motion but the pressure on the piston face is about a factor of 2 smaller than the pressure on the bottom of the cylinder. This behaviour, as we shall see, is intermediate between the strong and weak cases.

2.4. x-Velocity Distribution

At various times through the first descent of the piston we can examine the x-component of the velocity of each particle versus the x-component of its position (see Fig. 7). In the first plot at $t = 3.98$, immediately after the piston is released we observe a Maxwellian distribution of velocity components for all positions, except very near the piston face where a small band of large negative velocities occur due collisions with the descending piston. In the second plot the movement of the piston has increased this band of negative velocities, and again in the third plot. In the fourth plot the band of negative velocities has reached the bottom of the cylinder and there is some evidence of larger positive velocities due to collisions with the bottom of the cylinder. The process continues in the last two frames and there is a suggestion that the system has equilibrated to a new, higher temperature.

In the case of strong damping,[2] the piston behaves initially like a piston in an infinite cylinder and acquires almost immediately a stationary velocity $V = -8$. Since the velocity is constant the effective pressure is $Mg/L = 6.8$ (consistent with Fig. 6). To reverse the momentum of the piston, assuming that the time needed is about $t = 2$, requires pressure difference of $2MV/Lt \sim 1.7$ which is a small variation of the pressure on the piston. On the other hand when the piston reaches its minimum position the pressure on the bottom of the cylinder (taking the density 0.16 and a temperature 120) is 19. Then the piston almost immediately acquires a velocity $V = +8$ which means that the molecules with velocity less than 8 will not collide with it. Therefore the velocity distribution has an upper cut-off of 8 which represents a typical thermal velocity. Thus, after one cycle, the gas has increased its energy and the temperature to $kT = 40$ which corresponds to an average thermal velocity of around 9.

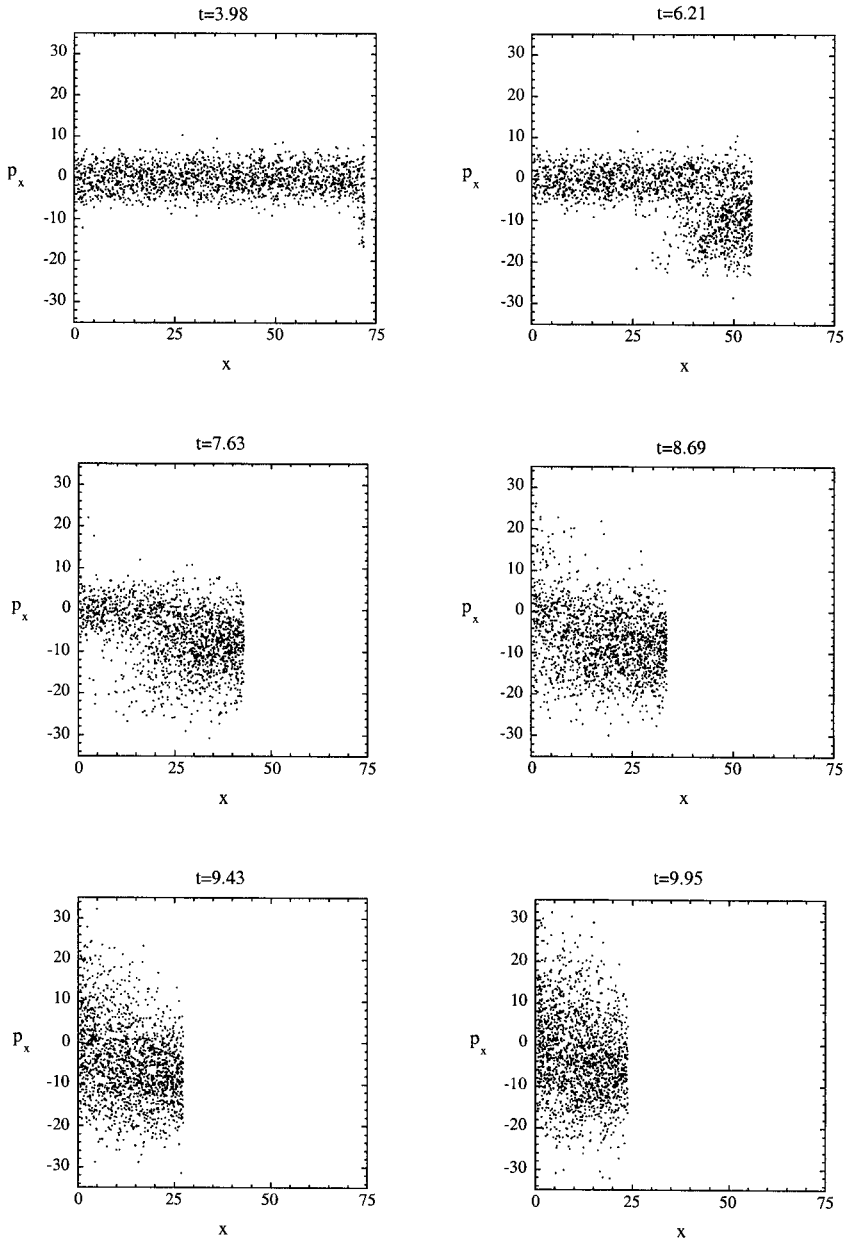

Fig. 7. The distribution of x-velocities as a function of the distance from the bottom of the cylinder. The piston is released at $t = 3.68$. In the first two frames the piston motion generates particles with large negative velocities, through collisions.

2.5. Weak Damping Case

Here the geometry is the same as that shown in Fig. 1, except for the change in piston mass and g (although the product Mg remains unchanged). Again the hard disk gas is first thermalised, the piston released at $t = 3.68$, and the simulation followed through time. In Fig. 8 is the graph of piston position versus the zeroth velocity moment and this figure is quite different from Fig. 3. There is a small straight segment, but both the clear damping and strong circular motion are not as evident as for the strong damping case. Indeed, for weak damping, fluctuations in j_0 have replaced the fluctuations in piston velocity of the strong damping case (see Figs. 3 and 8).

In Fig. 9 the motion of the piston is much smoother and there is little difference between the first two descents. Both the velocity and position change in a smooth but not sinusoidal way. Here most of the mass is in the piston ($M = 8000$) rather than the gas ($Nm = 1728$), and the quantity with the smallest mass shows the largest fluctuations.

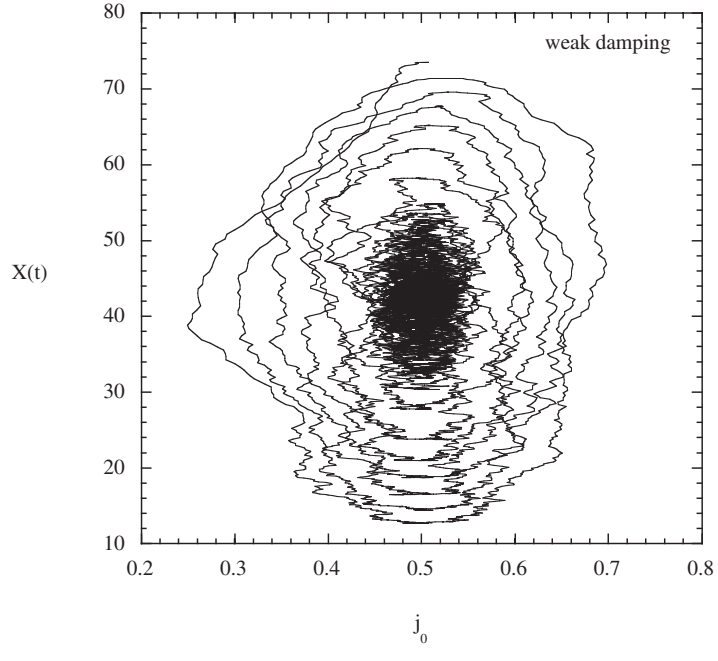

Fig. 8. The piston motion versus the zeroth velocity moment. Here the damping of the motion is evident but considerably slower than in Fig. 3.

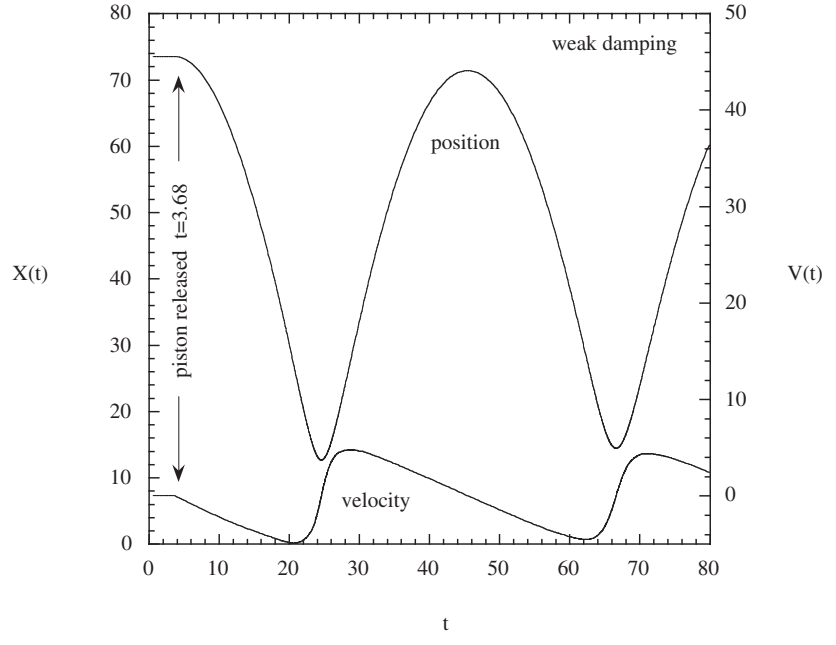

Fig. 9. The position and velocity of the piston as a function of time. The piston is released at $t = 3.68$ and reaches the bottom of its travel at $t = 24.62$. The piston slowly accelerates to $V = -5$ then quickly accelerates to $V = +5$. The velocity repeats this same pattern during the second cycle of the piston.

2.6. Number Density Profiles

There was no obvious evidence of a wave motion in this state. However, there is some evidence of a wave motion in the number density profiles with a wavefront at $X = 60$ at $t = 6.82$, and then at $X = 0$ at $t = 16.07$. This gives a wave velocity of ~ -6, and as the piston velocity decreases linearly from 0 to -5, the wave travels to the bottom of the cylinder well before the piston reaches the bottom of its travel. After the wave reaches the bottom of the cylinder the number density appears to increase uniformly as the piston descends, and the volume decreases. The change in number density profiles (Fig. 10) is not as dramatic as it was for the strong damping state (at most a factor of two, compared with a factor of three for strong damping). There is no evidence of the piston producing a significant number of particles with large negative velocities.

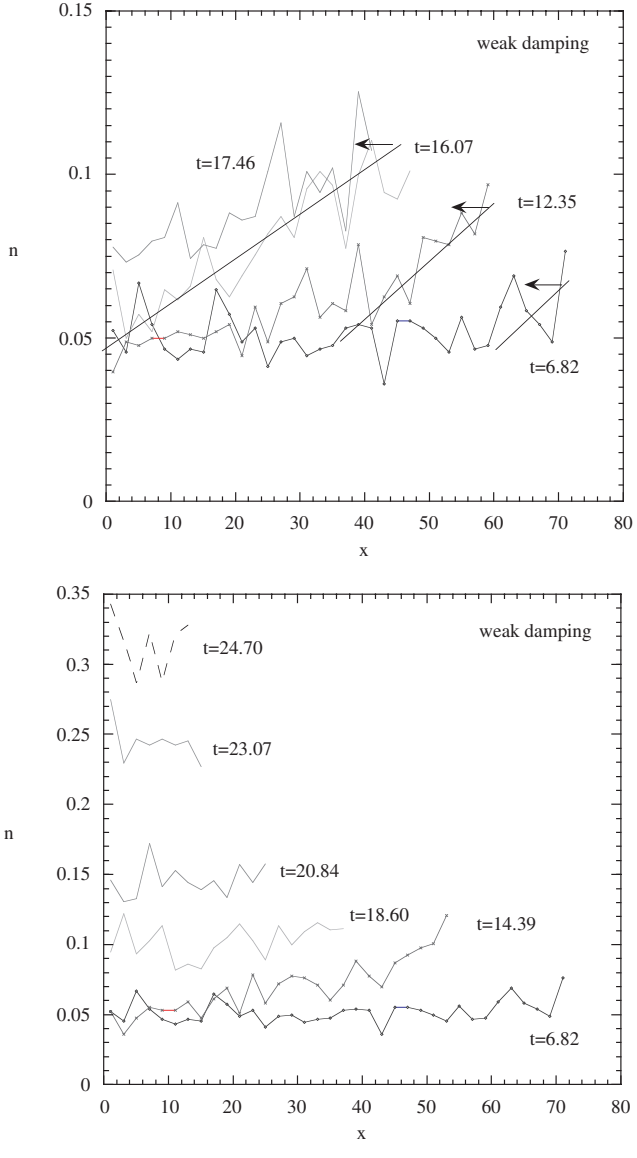

Fig. 10. The number density as a function of time through the first descent of the piston. The first plot shows evidence of some wave like motion with a velocity of about -6 but the amplitude is at most half that of the strong damping case. The second plot is the same simulation but over the full time period taken for the piston to reach its lowest point.

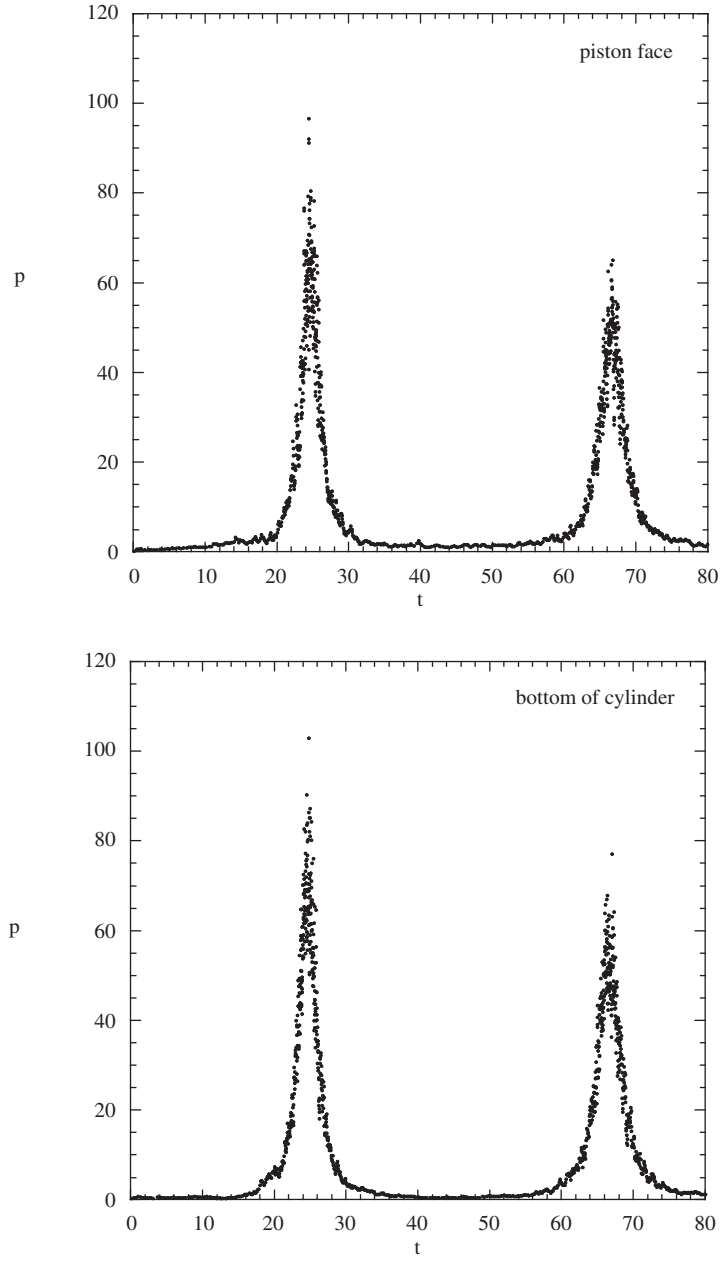

Fig. 11. The instantaneous pressures on the bottom of the cylinder and on the piston face are approximately equal throughout the motion of the piston.

2.7. Instantaneous Pressures

The instantaneous pressure on the piston surface and the bottom of the cylinder are almost the same, as a function of time (Fig. 11). The sharp peak in pressure occurs at the lowest point in the piston motion for both the first and second cycles of the piston motion, and the peak heights are indistinguishable. Clearly the pressure is uniform throughout the gas and the system is almost always in a state of mechanical equilibrium, which is entirely different from the strong damping case (Fig. 6).

2.8. x-Velocity Distribution

The x-components of velocity for the weak damping case in Fig. 12, do not show the same behaviour as we saw in the strong damping in Fig. 7. The motion of the piston is slower, so the distribution of velocities is not greatly effected in the first three frames. At $t = 20.84$ there is some suggestion of some small asymmetry of velocities but this appears to have equilibrated in the next two frames, at $t = 23.07$ and $t = 24.70$. Because the piston velocity is smaller, the time scale is longer, the velocities have more time to equilibrate.

In the case of weak damping, the piston only acquires a velocity $V = -5$ before turning around. In this case the effective pressure during the descent is strictly smaller than ~ 6.5. On the other hand the force per unit area necessary to reverse the velocity is now about $2MV/Lt \sim 85$ (which correspond to results in Fig. 11) while the pressure on the bottom is approximately 50 (using a density of 0.3 and a temperature of 120). Now the piston will acquire a velocity at most equal to $+5$ and thus all the molecules with velocity larger than 5 will hit the piston and loose energy. In this case, after one cycle the temperature of the gas increases to only $kT = 14$ which corresponds to an average thermal velocity of around 5.3.

3. CONCLUSIONS

As stated in the introduction, the final equilibrium state is very simple to find using thermostatics. It is precisely because we know the final answer that we want to understand whether there is an approach to this final state from a microscopic point of view. This simple model poses fundamental questions in statistical physics as one can see from.[8] It is in fact one of the problems mentioned by Lieb in his talk "Some problems in statistical mechanics that I would like to see solved." The question: "Does the piston evolve toward a stationary state?," has been discussed as an open problem

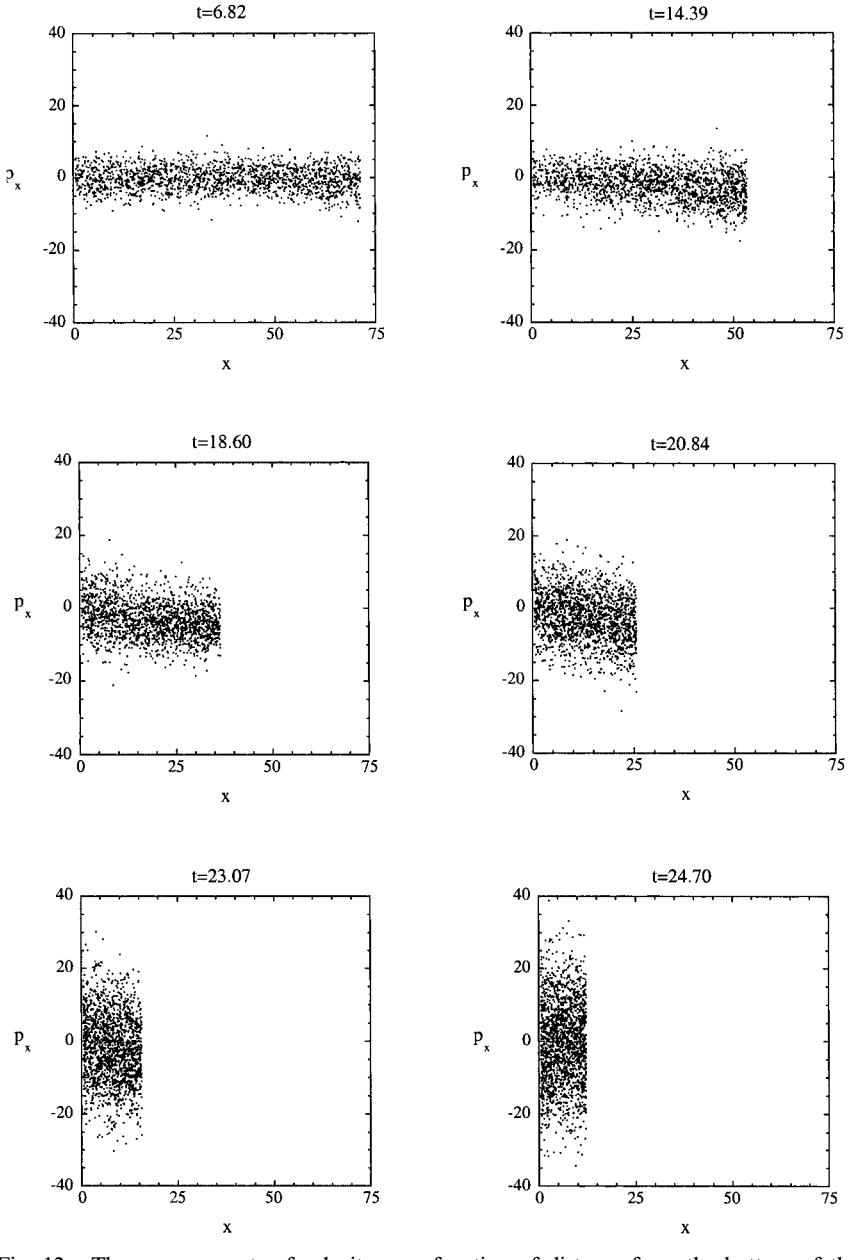

Fig. 12. The x-components of velocity as a function of distance from the bottom of the cylinder. This weak damping case looks like a relatively uniform compression of the gas leading to a steady rise in the temperature.

by Lebowitz *et al.*.[9] We show that for some values of the parameters considered here the oscillations can not be adiabatic which confirms the experimental results mentioned in the introduction. The frequency of the oscillations obtained with the adiabatic assumption coincide with the frequencies observed in the simulations only for weak damping. On the other hand the damping coefficient is entirely different.

Our results establish:

(i) The microscopic system evolves toward the equilibrium state predicted from thermostatics using as a state function the Enskog formula, i.e., our simulations provide some information on the question raised in the paper of Lebowitz *et al.*.[9] In particular using only conservative mechanics leads to the approach toward equilibrium. The adiabatic evolution of the simple piston that we have discussed is a strictly Hamiltonian system with constant total energy. In all cases we observe a damping mechanism, with either weak or strong damping. As the system is Hamiltonian and the phase space is bounded, the Poincaré recurrence theorem implies that the initial state should re-occur after some finite time.

(ii) It is observed within this model that two types of damping appear in the evolution toward the equilibrium state: strong damping and weak damping. This result is new in statistical mechanics and is confirmed by experiment. The simulations indicate how temperatures, pressures and density evolve as functions of time. Such information is of interest in order to obtain a realistic theoretical description. The mechanism that determines whether we observe weak or strong damping depends upon the speed of the piston relative to a typical thermal velocity of a gas particle in the cylinder. Under a given force the speed of the piston will be small if the ratio of the total mass of the fluid to the mass of the piston Nm/M is small; it will be large if this ratio is large. The key point is that as the piston rises up the cylinder after reaching its minimum position, only those gas particles whose velocity is greater than the velocity of the piston, can collide with it, and return some of their energy to the piston. This determines the flow of internal energy from the gas back to mechanical energy of the piston.

(iii) The damping coefficient is shown from the simulation to be very much different from the one predicted using simple kinetic theory together with some simplifying assumption. Indeed, in different regimes of the ratio of piston velocity to thermal velocity, the non-homogeneous nature of the fluid in the piston plays a decisive role in the character of the damping. In the case of weak damping the formulae for adiabatic oscillations gives a frequency of $\omega = 0.147$ (see ref. 7) while the observed value from the simulation is $\omega = 0.145$. On the other hand for strong damping one obtains $\omega = 1.324$ for adiabatic oscillations while the observed value is $\omega = 0.47$.

Therefore the assumption of adiabatic oscillations is not valid any more for strong damping, as was already observed in ref. 6. Moreover the difference between the observed value and the adiabatic case is much larger than the case discussed in ref. 6.

The other significant observation is that the size of the fluctuations observed in a component of the system (either the piston or the gas) is inversely proportional to the mass of that component. Indeed when the mass of the piston is large compared with the mass of the gas, as it is for the weak damping example, the piston moves smoothly, while j_0 (which is a gas property) has large fluctuations. In the strong damping example where the mass of the piston is smaller than the mass of the gas, the piston velocity has large fluctuations and j_0 varies relatively smoothly.

A more detailed kinetic theory analysis of the simple piston will be published elsewhere.[7]

ACKNOWLEDGMENTS

This paper is dedicated to Bob Dorfman whom it is an honour to regard as both a collaborator and a friend. G. Morriss greatly acknowledges the hospitality of the Institute of Theoretical Physics of the École Polytechnique Fédérale de Lausanne where this research was performed.

REFERENCES

1. H. B. Callen, *Thermodynamics* (Wiley, New York, 1963), Appendix C, see also Ch. Gruber, *Eur. J. Phys.* **20**:259–266 (1999).
2. Ch. Gruber and L. Frachebourg, *Phys. A* **272**:392–498 (1999).
3. Ch. Gruber, S. Pache, and A. Lesne, *J. Stat. Phys.* **108**:669–701 (2002).
4. Ch. Gruber, S. Pache, and A. Lesne, preprint 2002.
5. E. Rüchardt, *Phys. Z* **30**:58–59 (1929).
6. O. L. de Lange and J. Pierrus, *J. Chem. Phys.* **111**:1527–1532 (1999).
7. Ch. Gruber and G. P. Morriss, preprint 2002.
8. E. Lieb, *Phys. A* **263**:491 (1999).
9. J. L. Lebowitz, J. Piasecki, and Ya Sinai, Encyclopedia of mathematical science series **101**:217–227 (2000).